Design of experiment optimization of aligned polymer thermoelectrics doped by ion-exchange Ⓕ ⓢ⊙

ⓘD Yuxuan Huang, ⓘD Dionisius Hardjo Lukito Tjhe, ⓘD Ian E. Jacobs, et al.

COLLECTIONS

Paper published as part of the special topic on Organic and Hybrid Thermoelectrics

Ⓕ This paper was selected as Featured

ⓢ⊙ This paper was selected as Scilight

ARTICLES YOU MAY BE INTERESTED IN

Organic and hybrid thermoelectrics
Applied Physics Letters 119, 260401 (2021); https://doi.org/10.1063/5.0082126

Band mobility exceeding $10 \, cm^2 \, V^{-1} \, s^{-1}$ assessed by field-effect and chemical double doping in semicrystalline polymeric semiconductors
Applied Physics Letters 119, 013302 (2021); https://doi.org/10.1063/5.0052279

On the concept of an effective temperature Seebeck ratchet
Applied Physics Letters 119, 023303 (2021); https://doi.org/10.1063/5.0052116

Design of experiment optimization of aligned polymer thermoelectrics doped by ion-exchange

Yuxuan Huang,[1] Dionisius Hardjo Lukito Tjhe,[1] Ian E. Jacobs,[1] Xuechen Jiao,[2] Qiao He,[3] Martin Statz,[1,4]
Xinglong Ren,[1] Xinyi Huang,[5] Iain McCulloch,[6,7] Martin Heeney,[3] Christopher McNeill,[2]
and Henning Sirringhaus[1,a]

AFFILIATIONS

[1]Optoelectronics Group, Cavendish Laboratory, University of Cambridge, J J Thomson Avenue, Cambridge CB3 0HE,
United Kingdom
[2]Department of Materials Science and Engineering, Monash University, Wellington Road, Clayton, Victoria 3800, Australia
[3]Department of Chemistry and Centre for Processable Electronics, Imperial College London, London, United Kingdom
[4]Georg-August-Universität Göttingen, I. Physikalisches Institut, Friedrich-Hund-Platz 1, 37077 Göttingen, Germany
[5]School of Materials Science and Engineering, University of Shanghai for Science and Technology, Shanghai 200093, China
[6]KAUST Solar Center, Physical Sciences and Engineering Division (PSE), Materials Science and Engineering Program (MSE),
King Abdullah University of Science and Technology (KAUST), Thuwal, Kingdom of Saudi Arabia
[7]Department of Chemistry, University of Oxford, Oxford, United Kingdom

Note: This paper is part of the APL Special Collection on Organic and Hybrid Thermoelectrics.
[a]Author to whom correspondence should be addressed: hs220@cam.ac.uk

ABSTRACT

Organic thermoelectrics offer the potential to deliver flexible, low-cost devices that can directly convert heat to electricity. Previous studies have reported high conductivity and thermoelectric power factor in the conjugated polymer poly[2,5-bis(3-tetradecylthiophen-2-yl)thieno[3,2-b]thio-phene] (PBTTT). Here, we investigate the thermoelectric properties of PBTTT films in which the polymer chains were aligned uniaxially by mechanical rubbing, and the films were doped by a recently developed ion exchange technique that provides a choice over the counterions incorporated into the film, allowing for more optimized morphology and better stability than conventional charge transfer doping. To optimize the polymer alignment process, we took advantage of two Design of Experiment (DOE) techniques: regular two-level factorial design and central composite design. Rubbing temperature T_{rub} and post-alignment annealing temperature T_{anneal} were the two factors that were most strongly correlated with conductivity. We were able to achieve high polymer alignment with a dichroic ratio >15 and high electrical conductivities of up to 4345 S/cm for transport parallel to the polymer chains, demonstrating that the ion exchange method can achieve conductivities comparable/higher than conventional charge transfer doping. While the conductivity of aligned films increased by a factor of 4 compared to unaligned films, the Seebeck coefficient (S) remained nearly unchanged. The combination of DOE methodology, high-temperature rubbing, and ion exchange doping provides a systematic, controllable strategy to tune structure–thermoelectric property relationships in semiconducting polymers.

Conjugated polymers are promising candidates for thermoelectrics due to their low thermal conductivity and high Seebeck coefficients. However, in many materials, low electrical conductivity limits the thermoelectric figure of merit (ZT) and, therefore, real-world applications.[1–5] Improving electrical conductivity in these materials through improvements in film morphology and doping techniques is critical to the future success of organic thermoelectrics.[1,4] Charge transport in conjugated polymers tends to be fastest along the polymer backbone reflecting the intrinsic anisotropy of the electronic structure.[6–8] Hence, various methods to induce a uniaxial chain alignment along the direction of charge transport have been found effective to improve the charge transport and maximize the electric conductivity and thermoelectric properties. Some approaches achieved a particularly high degree of orientation, such as mechanical rubbing,[9–12] shear coating,[13,14] stretch alignment,[15,16] or epitaxy.[17,18] Among them, mechanical rubbing is one of the most versatile

methods to facilitate the crystallization and high-level orientation of conjugated polymers.[10,11]

Of similar importance is the choice of the doping method that is needed to induce a high concentration of mobile charge carriers in the polymer film after it has been aligned. One of the most commonly used methods for p-type doping involves exposing a solid polymer film to a solution of a charge transfer dopant with a high electron affinity[19,20] or depositing the charge transfer dopant onto the surface of the polymer by evaporation.[21–23] The dopant accepts an electron from the polymer, generating an anion, which is then incorporated into the film to provide the charge stabilizing counterions for the mobile polarons generated on the polymer. By combining polymer chain alignment by mechanical rubbing with charge transfer doping using $FeCl_3$, very high electrical conductivities of up to 10^5 S/cm have recently been reported for the conjugated polymer PBTTT.[11] However, the charge transfer doping technique has some clear limitations, in particular, the limited chemical stability of the dopant anions, which can lead to rapid degradation of the electrical conductivity of the doped films.

In this work, we use a recently developed ion-exchange (IEX) doping technique, which involves exposing the films to a solution comprising both a molecular dopant and an electrolyte.[24] The dopant induces the charge transfer as above, but the reduced dopant anion is not incorporated into the film. Instead, it exchanges with the negative ion of the electrolyte, which is chosen to be a chemically stable, closed shell ion. We have recently demonstrated that this technique is broadly applicable to a broad range of conjugated polymers, including PBTTT, and can achieve higher electrical conductivity than F4TCNQ or $FeCl_3$ doping without ion exchange.[25] Here, we apply this recent technique to PBTTT films aligned by mechanical rubbing and investigate the thermoelectric properties that can be achieved.

The fabrication process of aligned polymer films [Fig. 1(a)] involves a large number of process parameters that require optimization. The high dimensionality of the problem makes optimization time-consuming; therefore, researchers often focus on the impact of individual parameters like rubbing temperature T_{rub}[10] or the number of rubbing cycles.[9] The effect of many of these parameters on the resulting film is not obvious and is generally not included in the literature reports; additionally, they may interact with one another in non-trivial ways, preventing straightforward optimization of each parameter individually. To facilitate the optimization, we have used a Design of Experiment (DOE) approach, which is widely used as a statistical tool in industrial process development, such as pharmaceutical or biotechnology processes.[26–29] This allows for a systematic investigation of the key parameters that influence the high-temperature rubbing process. In our previous work, the ion-exchange doping process had been optimized with the combination of $FeCl_3$ and 1-butyl-1-methylpyrrolidinium bis(trifluoromethylsulfonyl)imide (BMP TFSI) for PBTTT, which leads to a complete bleaching of the PBTTT neutral absorption band and a high doping concentration on the order of 8×10^{20} cm^{-3} [Figs. 1(b) and 1(c)].[25] The same process is used in the optimization process without further modification.

The use of the DOE methodology provides several benefits [Fig. 2(a)]. First, DOE allows us to systematically investigate a large number of potentially key process parameters to maximize electrical conductivity and then combine each optimized parameter for an overall optimized process.[26–28] We conducted the optimization by varying all parameters simultaneously due to the potential cross correlation effects between rubbing parameters. At the outset, the key parameters for achieving alignment were not known; therefore, we considered all parameters that could conceivably affect alignment quality in our optimization, including stage speed, roller rotation and height, number of rubbing cycles, the temperature during rubbing T_{rub}, and the post-alignment annealing temperature T_{anneal} (Table I). The impact of the rubbing cloth types, side chain length of PBTTT, and film thickness on polymer crystallization and orientation was also considered in the later screening rounds. The DOE methodology allowed us to keep the experiments needed to identify an optimum in such a multi-dimensional design space to a reasonable number.
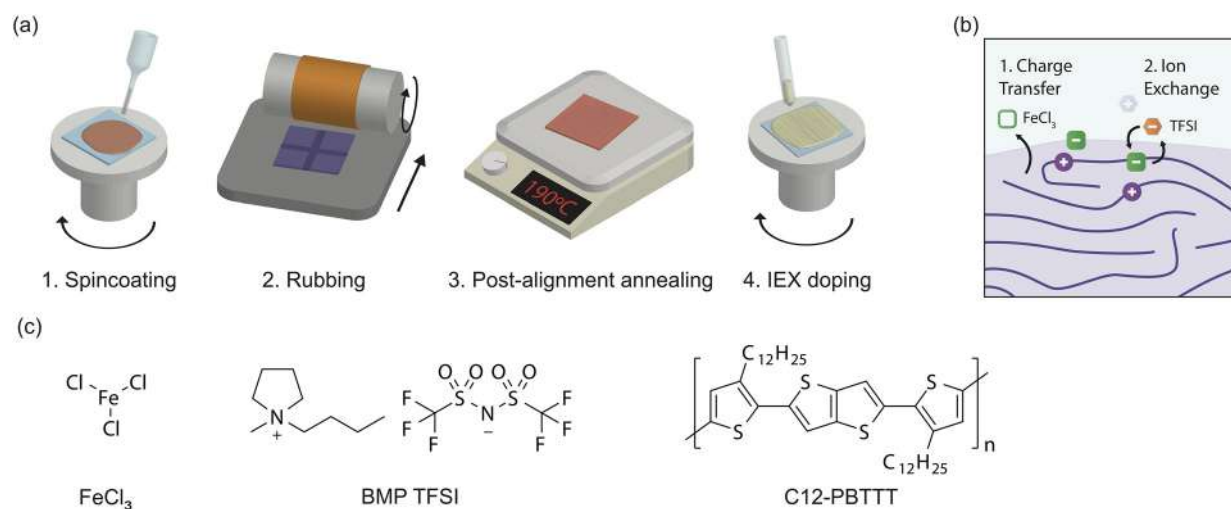

FIG. 1. (a) Preparation method of aligned, ion-exchange doped samples: spincoating, rubbing, post-alignment annealing, and ion-exchange doping. (b) Schematic of the ion-exchange doping process. (c) Chemical structure of $FeCl_3$, 1-butyl-1-methylpyrrolidinium bis(trifluoromethylsulfonyl)imide (BMP TFSI), and poly[2,5-bis(3-tetradecylthiophen-2-yl)thieno[3,2-b]thiophene] (C12-PBTTT).
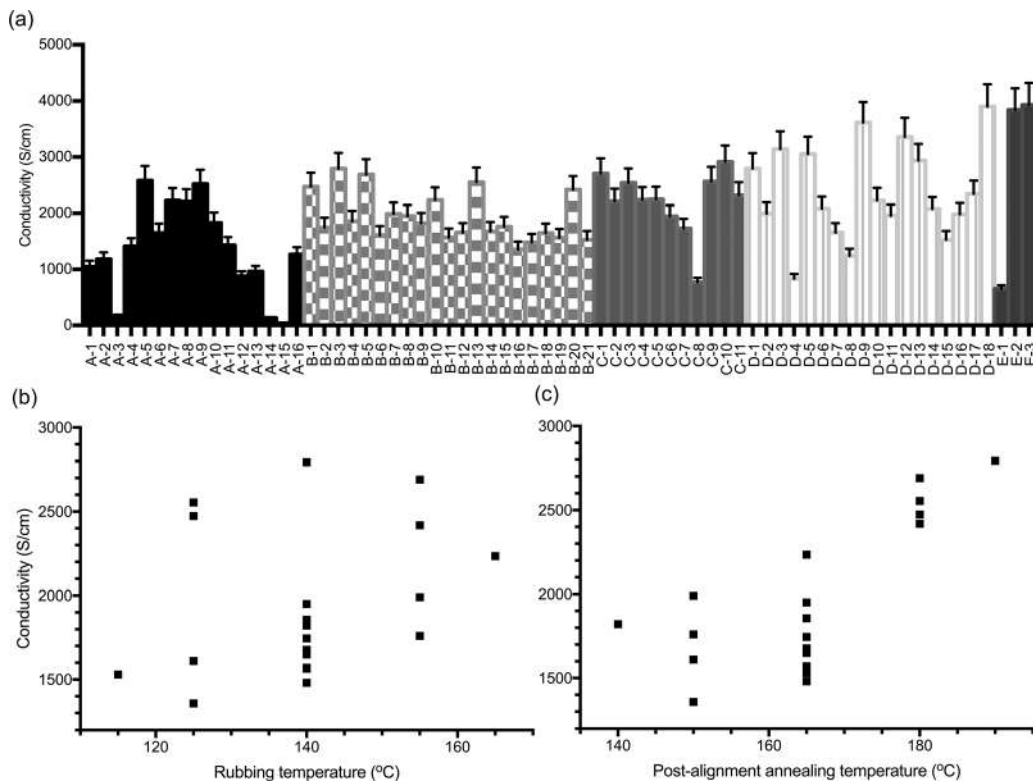
FIG. 2. (a) Conductivity results of aligned and doped C12-PBTTT from screening A to E, the evolution of conductivity as a function of (b) T_{rub}, and (c) T_{anneal} measured from screening B.

The first-round screening experiment, screening A, was designed using regular two-level factorial design. The purpose of the first-round screening was to screen the multidimensional factors to rule out insignificant rubbing factors and locate a maximum in conductivity to direct the next-level screening. The lower level of T_{rub}, 125 °C, was extracted from the previous studies,[10,11] while the higher T_{rub} at 180 °C was selected to be above the first phase transition in the differential scanning calorimetry (DSC) trace of PBTTT.[13] Both stage speed and roller rotation were set at the lowest (100 rpm) and highest (1500 rpm) values supported by our rubbing machine. (Note: stage

TABLE I. Parameters of film preparation and high-temperature rubbing in screening A–E.

Parameter	A	B	C	D	E	Optimum
Polymer	C14-PBTTT	C14-PBTTT	C14-PBTTT	C12-PBTTT	C12-PBTTT	C12-PBTTT
Cloth	Rayon	Rayon	Rayon	Microfiber cloth	Microfiber cloth	Microfiber cloth
Solution concentration (mg/ml)	10	10	10	20	10	10
Spin-coating speed (rpm)	1500	1500	1500	(500), 750, 1500, 3000, (8000)	600, 1000, 1500	1000
Rubbing temperature (°C)	125, 180	(115), 125, 140, 155, (165)	(132), 140, 160, 180, (188)	(115), 125, 140, 155	155	155
Stage speed (rpm)	100, 1500	(1200), 1300, 1400, 1500	1500	1500	1500	1500
Roller rotation speed (rpm)	100, 1500	(950), 1100, 1300, 1500	1500	1500	1500	1500
Rubbing cycles	0.5, 3	0.5	0.5	0.5	0.5	0.5
Post-alignment annealing temperature (°C)	RT, 180	(140), 150, 165, 180, (190)	(166), 180, 215, 250, (264)	RT, (163), 170, 180, 190, 197	190	190

speed is also set in rpm in our rubbing machine; 1500 rpm is approximately 0.8 cm/s.) The number of rubbing cycles, which may likely affect the dichroic ratio of orientated polymer films,[9] was set at either half a cycle or three cycles in screening A. Post-alignment annealing was previously reported to play a significant role in increasing the crystallinity and conductivity;[10] however, in previous work on the thermoelectric performance of rubbed PBTTT, the films did not undergo post-annealing.[11] Therefore, we tested both conditions without post-alignment annealing and with post-alignment annealing at $T_{anneal} = 180\,°C$. The DOE methodology required only 16 samples to characterize this five-dimensional design space in the pilot screening (Table I).

Among the 16 process routes in screening A (coded A-1 through A-16, Table S1 in the supplementary material for detailed parameters), the two top-performing samples, A-5 and A-9, resulted in higher conductivity than other results in this round (supplementary material, Table S1). There were two statistically significant factors, characterized by p-values (that is, the probability that the observed differences are due to random chance) lower than 0.05, from screening A: stage speed ($p = 0.0424$) and post-alignment annealing ($p = 0.0096$), as shown in the supplementary material, Table S2. In addition, the two optimum process routes in this round, A-5 and A-9, share common factors: higher roller rotation (1500 rpm), higher stage speed (1500 rpm), three rubbing cycles, and T_{anneal} at 180 °C; the only difference here is the higher T_{rub} at 180 °C for A-5 compared to T_{rub} at 125 °C for A-9.

The second-generation screening, screening B (coded B-1 to B-21 in the supplementary material, Table S1), was generated using a central composite design[28] with other parameter ranges extracted from model analysis of the first screening (supplementary material Table S1). Based on the first screening, we could rule out the potential effect from rubbing cycles, and then set at half cycle for the rest of optimization experiments. B-3 was the top-performing with an electric conductivity of 2793 S/cm among 21 process routes in screening B. A quadratic model with a p-value of 0.0083 (indicating strong predictive power) was used to fit the data from screening B (supplementary material, Table S3). Here, T_{rub} and T_{anneal} turn out to be the statistically significant factors controlling conductivity [Figs. 2(b) and 2(c)]; however, no cross correlation effects were considered to be statistically significant yet. Table S3 in the supplementary material contains an additional description of the statistical model.

The most apparent trend from screening B was that higher T_{anneal} resulted in higher conductivity, in particular, sample B-3 with the highest conductivity was annealed at the highest temperature of 190 °C in this round of screening [Fig. 2(c)]. Because the films are annealed before rubbing, this suggests that the alignment process may disrupt the film morphology, as we will address below. The effect of T_{rub} is likely more complex. Higher T_{rub} could promote the disentangling process of polymer backbones by promoting chain mobility, especially of the higher molecular-weight segments in the polydisperse polymer. However, if some of the thermal fluctuations of chain conformation that are present at high temperatures are frozen in when the films are cooled to room temperature, this could lead to enhanced disorder and lower conductivity, suggesting that there could be an optimum rubbing temperature.

The third-round screening, screening C (coded C-1 to C-11), was also generated by central composite design. Both stage speed and roller rotation were fixed in the previous round, 1500 rpm, as they were not found to be statistically significant factors in the previous round.

Instead, in this round, we focused on the higher temperature regime for both T_{rub} (132–188 °C) and T_{anneal} (166–264 °C) compared to screening B (Table I). The top-performing sample from this round is C-10 with a conductivity over 2900 S/cm with T_{rub} at 140 °C and T_{anneal} at 180 °C.

To further boost the electric conductivity of rubbed and doped PBTTT film after the previous three-round screenings, we then explored switching the side chain length of PBTTT to C12 and changing the rubbing cloth material from Rayon to a microfiber cloth (Table I).[10–12] In addition, we explored the influence of film thickness that may also affect the degree of crystallinity in conjugated polymer films.[30] Therefore, pristine PBTTT films of various thickness were prepared by spin-coating 20 mg/ml PBTTT solution at speeds ranging from 500 to 8000 rpm (Table I). We again varied T_{rub} from 125 to 155 °C, while T_{anneal} was varied from 163 to 190 °C in the screening D (coded D1–D18). Switching to C12-PBTTT and a microfiber cloth increased the conductivity up to the level of 3800 S/cm, while it appears that increasing the film thickness brings no significant advantage in conductivity enhancement.

Considering that spin coating from a high solution concentration may have produced non-uniform polymer films, we switched back to 10 mg/ml PBTTT solution and only varied polymer film spin coating speed at 600/1000/1500 rpm as the fifth and final screening. Spin coating of 10 mg/ml C12-PBTTT at 1000 rpm with T_{rub} at 155 °C and T_{anneal} at 190 °C (E-2, supplementary material, Table S1) was selected as the final conductivity-optimized rubbing process parameters, since no significant enhancement in electrical conductivity was achieved beyond the level of 3800–3900 S/cm.

Grazing incidence wide-angle x-ray scattering (GIWAXS) was performed on the films after the optimized rubbing process. The GIWAXS images in Fig. 3 show the high in-plane polymer chain alignment, inferred from the strong in-plane (010) π–π stacking peak and almost complete absence of the in-plane (003) backbone peak in the measurement parallel to the rubbing direction [Fig. 3(a)]. The inverse is seen in the same film measured perpendicular to the rubbing direction [Fig. 3(b)]. Without post-alignment annealing, we observe a predominantly face-on film texture (supplementary material, Fig. S1), consistent with previous reports.[11] In contrast, the annealed samples demonstrated much stronger out-of-plane (h00) reflections from edge-on crystalline population, with a smaller population of face-on crystallites, giving a broad distribution of in-plane (h00) reflections. Therefore, our findings suggest that while high-temperature rubbing tends to induce some face-on texture, post-alignment annealing largely returns the films to the edge-on texture observed in unaligned films [Fig. 3(c)]. This edge-on texture is generally beneficial for charge transport,[31] consistent with our findings that post-alignment annealing improves conductivity in doped films.

Polarized optical microscopy images [Figs. 4(a) and 4(b)] are also consistent with a very high degree of alignment. Remarkably, strong birefringence was observed when aligning the crossed polarizers at 45° to the rubbing direction, while near complete extinction was observed when the polarizers were aligned parallel/perpendicular to the rubbing direction [Figs. 4(a) and 4(b)]. The images provide clear evidence for a uniform and high level of chain alignment across the film, in good agreement with the GIWAXS data.

Polarized UV-VIS spectroscopy was used to monitor the degree of chain alignment before and after doping and quantify the dichroic
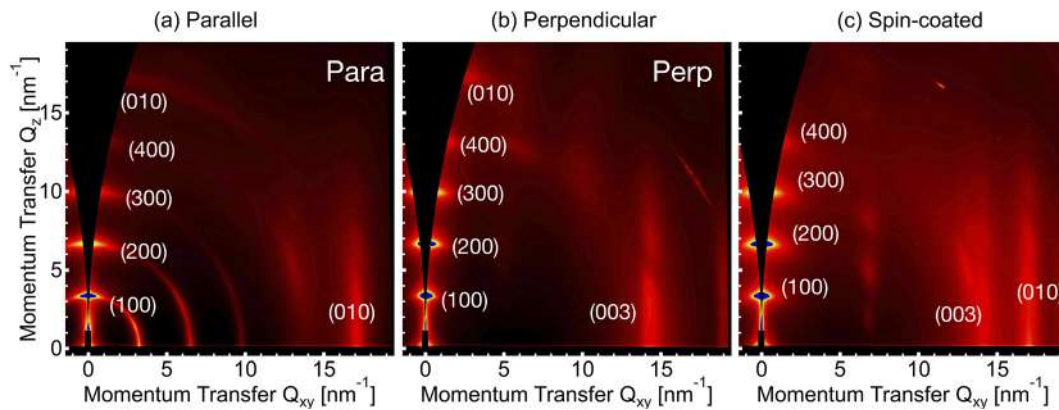
FIG. 3. Grazing incidence wide-angle x-ray scattering images of (a) and (b) PBTTT film prepared by the optimum process (parallel and perpendicular to rubbing direction) and (c) spin-coated before doping.

ratio and to monitor spectroscopically the level of polymer oxidation after doping [Fig. 4(c)]. The highly efficient ion-exchange doping by $FeCl_3$ and BMP TFSI[25] leads to a near complete bleaching of the neutral polymer absorption band at 558 nm. In the doped films, we observe instead the characteristic charge induced P2 (854 nm for 1 mM and 834 nm for 5 mM) and P1 (>1800 nm) absorption bands of oxidized PBTTT. We compare here two different doping concentrations of 1 and 5 mM that will be used below for thermoelectric characterization. With the polarizer parallel to the alignment direction, we find that in the 1 mM $FeCl_3$, ion-exchange doped sample P2 band is slightly higher than in the 5 mM sample, while the P1 band shows the opposite trend. This is likely to reflect slight differences in the electronic state delocalization of the polaronic charge carriers in the film.[25] From the polarized UV-VIS spectra, we can extract the dichroic

ratio defined as I_{max}/I_{min} [or alternatively as $(I_{max}-I_{min})/(I_{max} + I_{min})$, supplementary material, Fig. S2]. Notably, the dichroic ratio I_{max}/I_{min} reached the maximum value of 16.4 at 584 nm for undoped PBTTT, while in the doped samples, when using the P2 band at 910–920 nm, we extract slightly lower values of 11.1 (13.3) in the 1 (5) mM samples. This small drop in dichroic ratio of P2 band upon doping could indicate a loss of orientation upon intercalation of anions into the film. However, the P1 dichroic ratios of the doped sample are higher and continue increasing as we approach the low-energy limit of our measurements. In the 5 mM sample, the P1 dichroic ratio is slightly higher than that of the undoped polymer, suggesting that the P2 dichroic ratios may limited by scattering on the rough film surface generated by rubbing. This scattering gives rise to a background absorption signal in the perpendicular spectra similar in intensity to
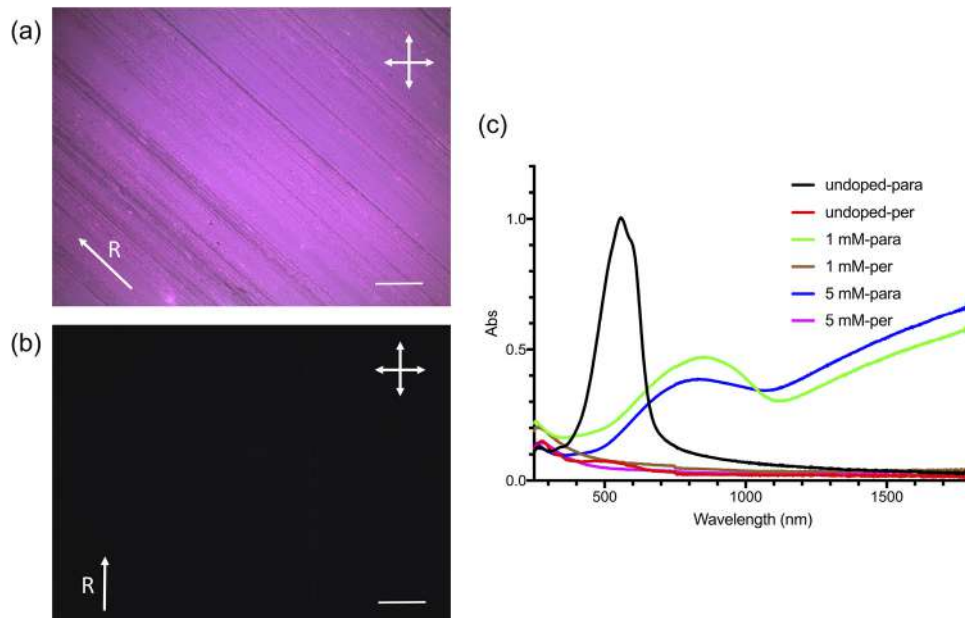

FIG. 4. (a) and (b) Polarized optical microscope images of aligned undoped PBTTT. Polarizer and analyzer orientations are shown as double arrows. The strong birefringence at 45° was observed. Scale bar: 400 μm. (c) Polarized UV-VIS spectra of undoped and doped PBTTT after high-temperature rubbing.

the P2 band, which makes it difficult to determine an accurate value of dichroic ratio at this high-level alignment where the P2 band can no longer be resolved. In any case, the UV-VIS data indicate clearly that the degree of alignment remains high after doping and is higher than the highly conducting PBTTT samples reported in Ref. 11. For both doped samples, we observe no residual $FeCl_{4-}$ anions, which would lead to an absorption signature at 367 nm.[25] This demonstrates the effectively complete exchange of dopants by $TFSI^-$ anions, consistent with our previous findings.

To assess the merits of our aligned PBTTT for thermoelectric applications, we investigated two representative samples with doping concentrations of 1 and 5 mM that gave high electrical conductivities. We previously observed that $FeCl_3$ dopant concentrations above 1 mM etched uncovered gold electrodes in a matter of minutes, forcing us to limit the dopant concentration to 1 mM. Here, we use Pt electrodes in the transport measurements, allowing us to increase the dopant solution concentration and achieve slightly higher doping levels. We measured electrical conductivity and Seebeck coefficient as a function of temperature using an on-chip microfabricated device architecture in which the polymer film is patterned into a Hall bar shape as detailed previously.[32–34] This design allows very accurate determination of the Seebeck coefficient and the electrical conductivity. It uses on-chip calibrated temperature sensors for the Seebeck measurements as well as four-point probe electrical conductivity measurements of the same film region (supplementary material, Fig. S3). We established that there was no significant degradation of the electrical conductivity of the polymer films during the Hall bar patterning. Compared to the unaligned samples, the electrical conductivity of the aligned samples in the parallel direction is enhanced by a factor of 3 to 4, and the perpendicular direction is suppressed to only around 0.1 of the value of the unaligned samples. The conductivity values of our samples reaching a maximum of 4345 S/cm in the parallel direction compare very favorably to recent reports on PBTTT thin films,[21,23–25,35] but they are lower than the very high values reported in Ref. 11. The reasons for this are unclear, particularly given that the dichroic ratio of our aligned films is comparable/higher than that of the samples in Ref. 11. In our previous study,[25] we also observed ion-exchange doped samples to exhibit higher conductivities than reference samples doped by traditional charge transfer doping with $FeCl_3$ as used in Ref. 11. We cannot exclude that further optimization of our aligned, ion-exchanged doped samples is possible, but we note that the conductivity measurements in Ref. 11 were performed on unpatterned films, which leads to less accurate estimates of conductivity than the Hall bar geometry used here, especially for high-conductivity samples in which the film conductance becomes comparable to that of the electrodes.

To extract some information on the charge transport physics, we also measured the conductivity and Seebeck coefficient as a function of temperature. For all samples and alignment conditions, a finite conductivity remains in the 0 K limit. For low temperatures of up to 30 K, the conductivity scales approximately as $T^{1/2}$, and some samples show metallic temperature dependence $d\sigma/dT < 0$ in the high-temperature regime of around 250 K. These features are traditionally taken to signify the presence of metallic states in the samples, as observed in doped polyacetylene[36] and polyaniline.[37] We adopt a model proposed by Kaiser and Graham[38] to extract some of the relevant transport parameters. Details of the models are discussed in the supplementary material, and the fits to our experimental data are shown as solid lines

in Fig. 5(a). From the fits, it is evident that the aligned polymers have a higher value of the Efros–Shklovskii variable-range hopping activation term T_0, which is also reflected by their lower normalized conductivity at low temperature $\sigma(T)/\sigma(250\,K)$ (supplementary material, Fig. S4). This suggests that rubbing though beneficial in terms of inducing polymer alignment also increases somewhat the degree of energetic disorder in the films, which is evident also in the less well-defined edge-on texture in the GIWAXS measurements.

The Seebeck coefficients of all samples vary linearly with temperature, obeying the Mott formula for metals, in agreement with a previous study on anion-exchange doped PBTTT.[35] Our Seebeck measurements do not show a significant dependence on the alignment direction amongst the six considered samples, consistent with previous reports in the doped PBTTT,[39] but contrasts with that of stretch aligned polyacetylene.[16] Whereas increasing conductivity through simply doping generally leads to a decrease in Seebeck coefficient due to the increase in carrier density,[40] alignment may promote the conductivity by improving the charge mobility.[41] This modification leaves the Seebeck coefficient virtually unchanged, suggesting that alignment is a promising approach to optimizing the power factor in organic thermoelectrics. Our results suggest that increasing the dopant concentration only leads to a moderate increase in the hole density beyond 1 mM $FeCl_3$, as evidenced by the comparable Seebeck coefficients. The parallel aligned samples doped with 1 and 5 mM $FeCl_3$ showed power factors of 109 and 137 $\mu m^{-2}\,K^{-1}$, respectively, at room temperature, a fivefold increase from their unaligned counterparts.

Given that figure of merit (ZT) is the crucial factor to evaluate the thermoelectric properties, it is necessary to consider the effect of alignment and doping on the thermal conductivity. We have not yet performed measurements of thermal conductivity, but we expect significant anisotropy in thermal transport between the parallel and perpendicular directions, arising from the differences in bonding character (van der Waals vs covalent) and electrical conductivity along each crystal axis. In our case of high electronic conductivity after doping and alignment, the electronic contribution to the thermal conductivity will likely be significant. In addition, alignment may also affect the phonon (lattice) contribution to the thermal conductivity by increasing phonon mean free path. Previous studies reported a factor of 2–3 enhancement in thermal conductivity for ultra-high molecular weight polyethylene (UHMWPE) along the chain axis (high degree of alignment) to the conventional textile materials.[42] We may expect a similar increase in the lattice thermal conductivity along the alignment direction, although no experimental data have been obtained yet. Since the electronic and lattice contributions to thermal conductivity should, therefore, be greater in aligned films, the increase in ZT will probably be smaller than the significant improvement in the power factor observed above.

In conclusion, we have demonstrated a controllable and systematic strategy for optimizing the parameters for aligning PBTTT by mechanical rubbing and identifying process conditions for maximizing the conductivity of ion-exchange doped samples. Our optimization approach based on the design of experiment methodology leads to a high degree of polymer alignment verified by both GIWAXS and polarized UV-VIS spectroscopy, and a fourfold increase in conductivity relative to spin-coated PBTTT films under the same condition of ion-exchange doping. In addition to this increase in conductivity, our careful temperature-dependent Seebeck measurements indicate that high-temperature rubbing does not strongly affect the Seebeck coefficient.
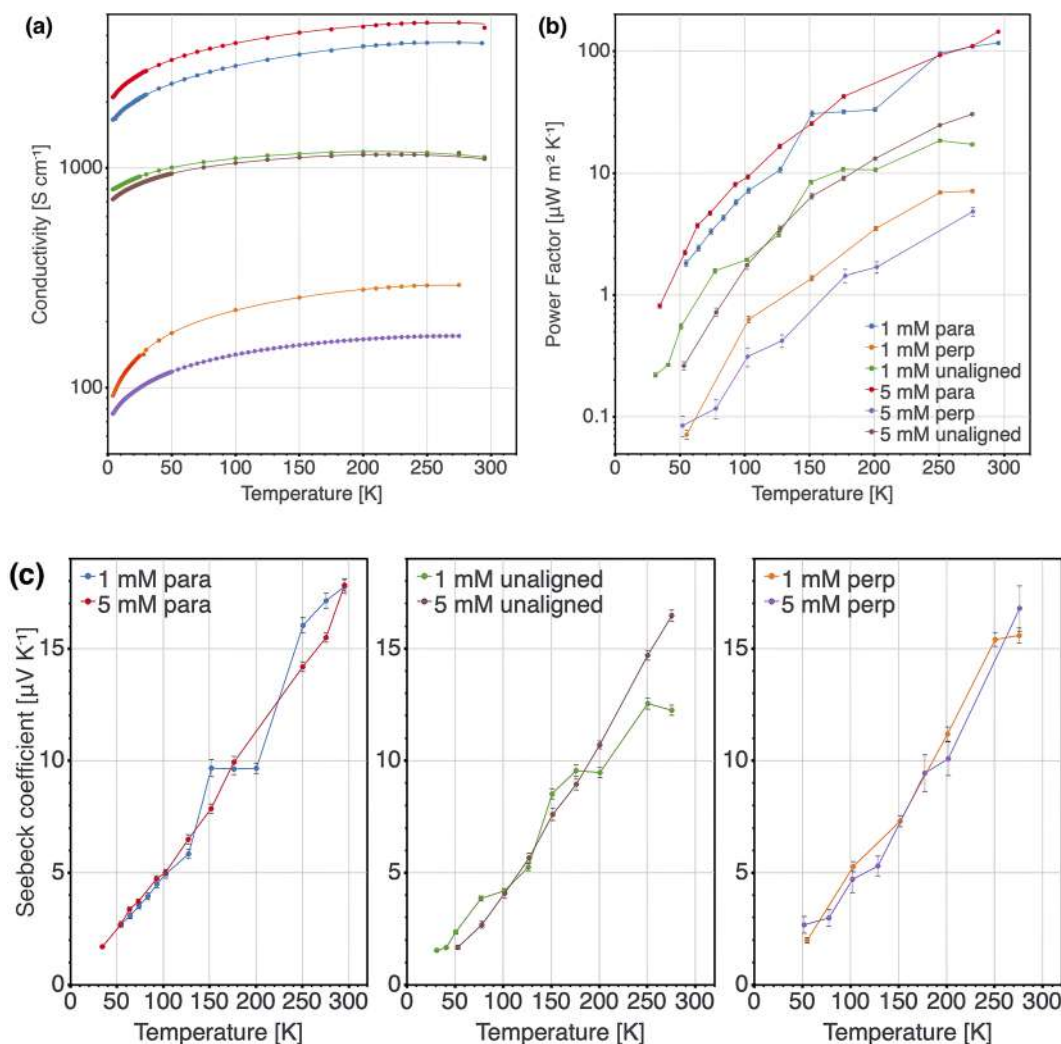
FIG. 5. (a) Temperature-dependent electrical conductivity, (b) power factor, and (c) Seebeck coefficient of the aligned and unaligned PBTTT films. The solid lines on panel (a) are fits according to Kaiser's model (see main text and the supplementary material, Fig. S4), while solid lines on panels (b) and (c) are guides for the eye. [(a) and (b) share the same plot colors].

The possibility of increasing conductivity uncoupled from the Seebeck coefficient provides a clear route for power factor enhancement. This opens the opportunities for further improving the microstructure of the mechanically rubbed polymer films, reducing their energetic disorder, and enhancing their thermoelectric performance. The DOE method applied here also simplifies performance optimization and should be widely applicable to other organic semiconductor devices.

See the supplementary material for more details on materials and methods, design of experiment optimization, additional characterization, and transport measurements.

DATA AVAILABILITY

The data that support the findings of this study are openly available at https://www.data.cam.ac.uk/repository.

REFERENCES

[1]R. Kroon, D. A. Mengistie, D. Kiefer *et al.*, "Thermoelectric plastics: From design to synthesis, processing and structure-property relationships," Chem. Soc. Rev. **45**(22), 6147–6164 (2016).

[2]B. Russ, A. Glaudell, J. J. Urban et al., "Organic thermoelectric materials for energy harvesting and temperature control," Nat. Rev. Mater. **1**(10), 16050 (2016).

[3]T. O. Poehler and H. E. Katz, "Prospects for polymer-based thermoelectrics: State of the art and theoretical analysis," Energy Environ. Sci. **5**(8), 8110–8115 (2012).

[4]Q. Zhang, Y. M. Sun, W. Xu et al., "Organic thermoelectric materials: Emerging green energy materials converting heat to electricity directly and efficiently," Adv. Mater. **26**(40), 6829–6851 (2014).

[5]O. Bubnova and X. Crispin, "Towards polymer-based organic thermoelectric generators," Energy Environ. Sci. **5**(11), 9345–9362 (2012).

[6]K. Tremel, F. S. U. Fischer, N. Kayunkid et al., "Charge transport anisotropy in highly oriented thin films of the acceptor polymer P(NDI2OD-T2)," Adv. Energy Mater. **4**(10), 1301659 (2014).

[7]X. Xue, G. Chandler, X. R. Zhang et al., "Oriented liquid crystalline polymer semiconductor films with large ordered domains," ACS Appl. Mater. Interfaces **7**(48), 26726–26734 (2015).

[8]A. Hamidi-Sakr, L. Biniek, S. Fall et al., "Precise control of lamellar thickness in highly oriented regioregular poly(3-hexylthiophene) thin films prepared by high-temperature rubbing: Correlations with optical properties and charge transport," Adv. Funct. Mater. **26**(3), 408–420 (2016).

[9]L. Hartmann, K. Tremel, S. Uttiya et al., "2D versus 3D crystalline order in thin films of regioregular poly(3-hexylthiophene) oriented by mechanical rubbing and epitaxy," Adv. Funct. Mater. **21**(21), 4047–4057 (2011).

[10]L. Biniek, S. Pouget, D. Djurado et al., "High-temperature rubbing: A versatile method to align pi-conjugated polymers without alignment substrate," Macromolecules **47**(12), 3871–3879 (2014).

[11]V. Vijayakumar, Y. H. Zhong, V. Untilova et al., "Bringing conducting polymers to high order: Toward conductivities beyond 10^5 S cm^{-1} and thermoelectric power factors of 2 mW m^{-1} K^{-2}," Adv. Energy Mater. **9**(24), 1900266 (2019).

[12]L. Biniek, N. Leclerc, T. Heiser et al., "Large scale alignment and charge transport anisotropy of pBTTT films oriented by high temperature rubbing," Macromolecules **46**(10), 4014–4023 (2013).

[13]D. M. DeLongchamp, R. J. Kline, Y. Jung et al., "Controlling the orientation of terraced nanoscale 'ribbons' of a poly(thiophene) semiconductor," ACS Nano **3**(4), 780–787 (2009).

[14]G. Giri, E. Verploegen, S. C. B. Mannsfeld et al., "Tuning charge transport in solution-sheared organic semiconductors using lattice strain," Nature **480**(7378), 504–508 (2011).

[15]B. O'Connor, R. J. Kline, B. R. Conrad et al., "Anisotropic structure and charge transport in highly strain-aligned regioregular poly(3-hexylthiophene)," Adv. Funct. Mater. **21**(19), 3697–3705 (2011).

[16]W. Pukacki, J. Plocharski, and S. Roth, "Anisotropy of thermoelectric-power of stretch-oriented new polyacetylene," Synth. Met. **62**(3), 253–256 (1994).

[17]M. Brinkmann and P. Rannou, "Molecular weight dependence of chain packing and semicrystalline structure in oriented films of regioregular poly(3-hexylthiophene) revealed by high-resolution transmission electron microscopy," Macromolecules **42**(4), 1125–1130 (2009).

[18]M. Brinkmann and J. C. Wittmann, "Orientation of regioregular poly(3-hexylthiophene) by directional solidification: A simple method to reveal the semicrystalline structure of a conjugated polymer," Adv. Mater. **18**(7), 860 (2006).

[19]I. E. Jacobs, E. W. Aasen, J. L. Oliveira et al., "Comparison of solution-mixed and sequentially processed P3HT:F4TCNQ films: Effect of doping-induced aggregation on film morphology," J. Mater. Chem. C **4**(16), 3454–3466 (2016).

[20]I. E. Jacobs, J. Li, S. L. Burg et al., "Reversible optical control of conjugated polymer solubility with sub-micrometer resolution," ACS Nano **9**(2), 1905–1912 (2015).

[21]S. N. Patel, A. M. Glaudell, K. A. Peterson et al., "Morphology controls the thermoelectric power factor of a doped semiconducting polymer," Sci. Adv. **3**(6), e1700434 (2017).

[22]E. Lim, K. A. Petersonm, G. M. Su et al., "Thermoelectric properties of poly(3-hexylthiophene) (P3HT) doped with 2,3,5,6-tetrafluoro-7,7,8,8-tetracyanoquinodimethane (F(4)TCNQ) by vapor-phase infiltration," Chem. Mater. **30**(3), 998–1010 (2018).

[23]E. M. Thomas, K. A. Petersonm, A. H. Balzer et al., "Effects of counter-ion size on delocalization of carriers and stability of doped semiconducting polymers," Adv. Electron. Mater. **6**(12), 2000595 (2020).

[24]Y. Yamashita, J. Tsurumi, M. Ohno et al., "Efficient molecular doping of polymeric semiconductors driven by anion exchange," Nature **572**(7771), 634 (2019).

[25]I. E. Jacobs, Y. Lin, Y. Huang et al., "High efficiency ion exchange doping of conducting polymers," Adv. Mater. (2021).

[26]K. J. Kauffman, J. R. Dorkin, J. H. Yang et al., "Optimization of lipid nanoparticle formulations for mRNA delivery in vivo with fractional factorial and definitive screening designs," Nano Lett. **15**(11), 7300–7306 (2015).

[27]L. Miao, L. Li, Y. Huang et al., "Delivery of mRNA vaccines with heterocyclic lipids increases anti-tumor efficacy by STING-mediated immune cell activation," Nat. Biotechnol. **37**(10), 1174 (2019).

[28]B. Gu, B. Linehan, and Y. C. Tseng, "Optimization of the Buchi B-90 spray drying process using central composite design for preparation of solid dispersions," Int. J. Pharm. **491**(1–2), 208–217 (2015).

[29]B. Cao, L. A. Adutwum, A. O. Oliynyk et al., "How to optimize materials and devices via design of experiments and machine learning: Demonstration using organic photovoltaics," ACS Nano **12**(8), 7434–7444 (2018).

[30]L. H. Jimison, S. Himmelberger, D. T. Duong et al., "Vertical confinement and interface effects on the microstructure and charge transport of P3HT thin films," J. Polym. Sci. Part B **51**(7), 611–620 (2013).

[31]K. Kang, S. Watanabe, K. Broch et al., "2D coherent charge transport in highly ordered conducting polymers doped by solid state diffusion," Nat. Mater. **15**(8), 896 (2016).

[32]M. Statz, S. Schneider, F. Berger et al., "Charge and thermoelectric transport in polymer-sorted semiconducting single-walled carbon nanotube networks," ACS Nano **14**(11), 15552–15565 (2020).

[33]C. N. Warwick, D. Venkateshvaran, and H. Sirringhaus, "Accurate on-chip measurement of the Seebeck coefficient of high mobility small molecule organic semiconductors," APL Mater. **3**(9), 096104 (2015).

[34]M. Statz, D. Venkateshvaran, X. Jiao et al., "On the manifestation of electron-electron interactions in the thermoelectric response of semicrystalline conjugated polymers with low energetic disorder," Commun. Phys. **1**, 16 (2018).

[35]S. Watanabe, M. Ohno, Y. Yamashita et al., "Validity of the Mott formula and the origin of thermopower in pi-conjugated semicrystalline polymers," Phys. Rev. B **100**(24), 241201 (2019).

[36]R. Zuzok, A. B. Kaiser, W. Pukacki et al., "Thermoelectric-power and conductivity of iodine-doped new polyacetylene," J. Chem. Phys. **95**(2), 1270–1275 (1991).

[37]P. N. Adams, P. Devasagayam, S. J. Pomfret et al., "A new acid-processing route to polyaniline films which exhibit metallic conductivity and electrical transport strongly dependent upon intrachain molecular dynamics," J. Phys. **10**(37), 8293–8303 (1998).

[38]A. B. Kaiser and S. C. Graham, "Temperature-dependence of conductivity in metallic polyacetylene," Synth. Met. **36**(3), 367–380 (1990).

[39]D. Scheunemann, V. Vijayakumar, H. Zeng et al., "Rubbing and drawing: Generic ways to improve the thermoelectric power factor of organic semiconductors?," Adv. Electron. Mater. **6**(8), 2000218 (2020).

[40]S. D. Kang and G. J. Snyder, "Charge-transport model for conducting polymers," Nat. Mater. **16**(2), 252–257 (2017).

[41]S. Schott, E. Gann, L. Thomsen et al., "Charge-transport anisotropy in a uniaxially aligned diketopyrrolopyrrole-based copolymer," Adv. Mater. **27**(45), 7356 (2015).

[42]A. A. Candadai, J. A. Weibel, and A. M. Marconnet, "Thermal conductivity of ultrahigh molecular weight polyethylene: From fibers to fabrics," ACS Appl. Polym. Mater. **2**(2), 437–447 (2020).